XXI IMEKO World Congress "Measurement in Research and Industry"
August 30 – September 4, 2015, Prague, Czech Republic

EVALUATION OF THE UNCERTAINTY OF GAS FLOW MEASUREMENTS BY A CLEARANCE-SEALED PISTON PROVER

Gregor Bobovnik, Jože Kutin, Ivan Bajsić

Laboratory of Measurements in Process Engineering, Faculty of Mechanical Engineering, University of Ljubljana, Aškerčeva 6, SI-1000 Ljubljana, Slovenia, email: gregor.bobovnik@fs.uni-lj.si

Abstract – A piston prover measures the flow rate by determining the time interval that a piston needs to pass a known volume of gas at a defined pressure and a temperature. The evaluation of the calibration and measurement capabilities of the clearance-sealed realization of the piston prover is presented. A systematic analysis of the uncertainty covers the components due to the gas density, dimensional and time measurements, the leakage flow, the density correction factor and the repeatability.

Keywords: piston prover, gas, mass flow rate, measurement uncertainty, CMC

1. INTRODUCTION

The piston-prover concept is widely used for primary standards in the field of gas flow measurements [1–10]. The general principle of operation is based on determining the time interval that a piston needs to pass a known volume of gas at a defined pressure and temperature. A general model for the mass flow rate reads as:

$$q_m = \rho_{m,2}\frac{V_m}{\Delta t} + \left(\rho_{d,2} - \rho_{d,1}\right)\frac{V_d}{\Delta t} + q_{m,l}\,, \qquad (1)$$

where V_m is the measuring volume of gas collected by the piston prover during the $\Delta t = t_2 - t_1$ interval, $\rho_{m,2}$ is the mean density of the gas in the measuring volume at the time t_2, V_d is the connecting volume of the gas between the meter under test and the piston at the time t_1, $(\rho_{d,2} - \rho_{d,1})$ is the change in the mean density of the gas in the connecting volume during the Δt interval, and $q_{m,l}$ is the leakage mass flow rate.

This article deals with a commercially available, high-speed, clearance-sealed realization of the piston prover [11,12], which is schematically shown in Fig. 1. In our previous work [13–15], we identified deficiencies of the measurement model originally employed in the piston prover and proposed some modifications. The purpose of this article is the systematic evaluation of the calibration and measurement capability (CMC) of such piston prover. The employed measurement model and its main assumptions are given in Section 2. Section 3 presents the evaluation of the uncertainty of the mass flow rate including the description of the main influential quantities and the methods for their estimation. The uncertainty analysis is presented for a flow cell with the flow range between 0.6 g/min and 60 g/min of dry air in ambient conditions. The analysis follows JCGM 100:2008 [16].

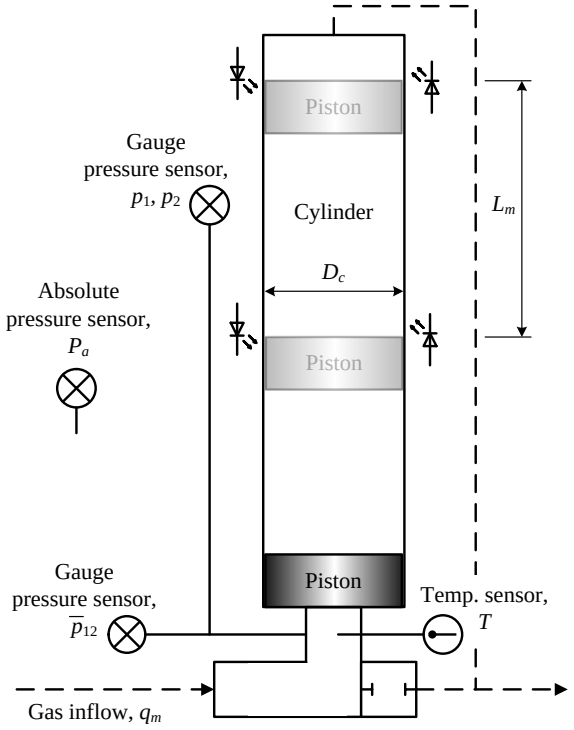

Fig. 1. Scheme of the clearance-sealed piston prover.

2. MEASUREMENT MODEL

The measurement model employed in the piston prover under discussion can be written as:

$$q_m = \rho\left(P_a, T\right)\left(\frac{V_m^*}{\Delta t} + q_{v,l}^{(p)}\right)\varepsilon_\rho\,. \qquad (2)$$

Nominal gas density $\rho(P_a,T)$ at the atmospheric pressure P_a and time-averaged gas temperature in the piston prover T is calculated using the equation for the real gas:

$$\rho\left(P_a, T\right) = \frac{P_a}{Z\left(R/M\right)T}\,, \qquad (3)$$

where Z is the compressibility factor, R is the universal gas constant and M is the molar mas of gas. The effective measuring volume V_m^* is expressed as

$$V_m^* = L_m \frac{\pi(D+\delta)^2}{4}, \quad (4)$$

where L_m is the distance passed by the piston in the time interval Δt, D is the piston diameter and $D + \delta$ is the effective diameter of the cylinder, where δ is the clearance thickness. The cylinder diameter is reduced from $D + 2\delta$ to $D + \delta$ to account for the Couette leakage flow component, which arises due to the piston movement relative to the cylinder wall. The Poisseuille leakage flow rate $q_{v,l}^{(p)}$ is determined experimentally using the dynamic summation method (see Section 3.3). Density correction factor ε_ρ accounts for variations of the gas density relative to $\rho(P_a,T)$. Considering the improved, adiabatic model that accounts for a quasi-adiabatic nature of relatively high-frequency oscillations of the gas, the correction factor reads as [13,14]:

$$\varepsilon_\rho^{(A)} = 1 + \frac{\overline{p}_{12}}{P_a} + \frac{1}{\gamma}\left(\frac{p_2 - \overline{p}_{12}}{P_a} + \frac{p_2 - p_1}{P_a}\frac{V_d}{V_m^*}\right). \quad (5)$$

where p_1 and p_2 are the gauge pressures at times t_1 and t_2, respectively, $\overline{p}_{12}$ is the time-averaged value of the gauge pressure during the timing cycle and γ is the adiabatic index. In the uncertainty analysis, the adiabatic model will be also compared to the isothermal model:

$$\varepsilon_\rho^{(T)} = 1 + \frac{p_2}{P_a} + \frac{p_2 - p_1}{P_a}\frac{V_d}{V_m^*}, \quad (6)$$

which is originally employed in the piston prover.

The measurement model (2-5) can be derived from the general model (1) using the following assumptions: spatially homogenous gas density in V_m and V_d at each time instant, $\rho_1 = \rho_{d,1}$ and $\rho_2 = \rho_{m,2} = \rho_{d,2}$, a thermal equilibrium between the inlet gas flow and the wall of the cylinder and negligible gas compressibility effects in the density correction factor, $Z_1 = Z_2 = Z_a$.

3. EVALUATION OF UNCERTAINTY

The presented uncertainty analysis of the mass flow rate of the dry air at ambient conditions covers the components due to the gas density, dimensional and time measurements, the leakage flow, the density correction factor and the repeatability. The methods applied for their estimation are also discussed.

3.1. Nominal gas density

The gas density is calculated using REFPROP database [17]. The components of the standard relative uncertainty of the gas density and their numerical values are presented in Table 1.

The absolute pressure is measured using the barometric sensor and the temperature is measured using the temperature sensor at the inlet of the cylinder (see Fig. 1). Their uncertainties are determined upon the calibration results and the calibration history (time drift). The contribution of the compressibility factor, which is pressure and temperature dependent, represents the uncertainty of the underlying REFPROP models and is estimated by a comparison of its values with those of certain reference model (e.g. CIPM-2007 formula for air [18]). The molar mass is on the other hand affected by the actual composition of the gas applied in a measurement process (e.g. amount of CO_2 and water vapour in air).

Table 1. Components of the gas density uncertainty, $u(\rho)/\rho = \sqrt{\sum_i \left(c_{rel,i}\, u(x_i)/x_i\right)^2}$

x_i	$c_{rel,i}\, u(x_i)/x_i$	$c_{rel,i}\, u(x_i)/x_i$ in %
P_a	$u(P_a)/P_a$	0.028
T	$-u(T)/T$	-0.026
Z	$-u(Z)/Z$	0.010
M	$u(M)/M$	0.011
$u(\rho)/\rho$		0.041

3.2. Dimensional and time measurements

The term $V_m^*/\Delta t$ depends on the dimensional quantities of the piston and the cylinder (D, L_m, δ) and the measurement time interval Δt. Time is measured using the internal time base. The uncertainties of the respective quantities are determined using the calibration results and the calibration history where applicable. More details about the estimation of the clearance thickness uncertainty, $u(\delta)$, can be found in [11]. The components of the relative standard uncertainty of the uncorrected volume flow rate (considering $\delta << D$ in the notation of the sensitivity coefficients), together with the estimated numerical values, are shown in Table 2. The values of the dimensional parameters are equal to: $D = 4.4430$ cm, $L_m = 7.6182$ cm and $\delta = 0.000889$ cm. The measurement time interval for a specific mass flow rate can be calculated using the measurement model (2).

Table 2. Components of the uncorrected volume flow uncertainty, $u(V_m^*/\Delta t)/(V_m^*/\Delta t) = \sqrt{\sum_i \left(c_{rel,i}\, u(x_i)/x_i\right)^2}$

x_i	$c_{rel,i}\, u(x_i)/x_i$	$c_{rel,i}\, u(x_i)/x_i$ in %
L_m	$u(L_m)/L_m$	0.007
D	$2u(D)/D$	0.025
δ	$2u(\delta)/D$	0.004
Δt	$-u(\Delta t)/\Delta t$	-0.018
$u(V_m^*/\Delta t)/(V_m^*/\Delta t)$		0.032

3.3. Leakage flow rate

The Poisseuille leakage flow rate is experimentally determined by the dynamic summation method. A gas is supplied by two stable mass flow controllers to two parallel flow branches, each restricted by a valve, which reunite before the inlet to the piston prover. The flow is measured with the piston prover from each flow branch separately by closing the valve in the other branch, as well as from both

branches simultaneously. The leakage flow rate is determined by subtracting the two flow rates obtained in the separate measurements of flow through each branch from the flow rate obtained for the both branches simultaneously. The uncertainty of the leakage volume flow rate $u(q_{v,l}^{(p)})$ is estimated using the experimental standard deviation of repeated measurements and the estimated temporal stability of the leakage flow rate. For the flow cell under consideration the leakage flow rate equals $q_{v,l}^{(p)} = 0.78\ \mathrm{cm^3/min}$ and its estimated standard uncertainty $u(q_{v,l}^{(p)}) = 0.15\ \mathrm{cm^3/min}$.

3.4. Density correction factor

The detailed uncertainty analysis of the density correction factors for the adiabatic and the isothermal models was presented in [14]. In Table 3, the significant components of the standard uncertainty are given for the adiabatic model (considering $\varepsilon_\rho \approx 1$ in the notation of the sensitivity coefficients). Additional uncertainty component $u(\varepsilon_\rho^{\Delta T})$ represents the heat exchange effect, which arises due to the temperature difference between the temperatures of the inlet gas flow and the cylinder wall (see [15] for more details).

Table 3. Components of the density correction factor uncertainty,

$$u(\varepsilon_\rho)/\varepsilon_\rho = \sqrt{\sum\nolimits_i \left(c_{rel,i}\, u(x_i)/x_i\right)^2}$$

x_i	$c_{rel,i}\, u(x_i)/x_i$
p_1	$-\frac{1}{\gamma}\frac{V_d}{V_m^*}\frac{p_1}{P_a}\frac{u(p_1)}{p_1}$
p_2	$\frac{1}{\gamma}\left(1+\frac{V_d}{V_m^*}\right)\frac{p_2}{P_a}\frac{u(p_2)}{p_2}$
$\overline{p}_{12}$	$\frac{\gamma-1}{\gamma}\frac{\overline{p}_{12}}{P_a}\frac{u(\overline{p}_{12})}{\overline{p}_{12}}$
V_d	$\frac{p_2-p_1}{\gamma P_a}\frac{V_d}{V_m^*}\frac{u(V_d)}{V_d}$
γ	$-\frac{1}{\gamma}\left(\frac{p_2-\overline{p}_{12}}{P_a}+\frac{p_2-p_1}{P_a}\frac{V_d}{V_m^*}\right)\frac{u(\gamma)}{\gamma}$
ΔT	$u\left(\varepsilon_\rho^{\Delta T}\right)$

The pressures p_1 and p_2 were measured using the piston prover's internal pressure sensor with the estimated standard uncertainty of $u(p_1) = u(p_2) = 5\ \mathrm{Pa}$, whereas the time-averaged pressure $\overline{p}_{12}$ is measured by the external pressure sensor (Validyne P855 & National Instruments USB-6251 BNC DAQ module) with the estimated standard uncertainty of $u(\overline{p}_{12}) = 2\ \mathrm{Pa}$. Fig. 2 shows the measured values of pressures p_1, p_1 and $\overline{p}_{12}$ in the timing cycles (scatter plots) at seven different flow rates and their approximations by second-order polynomials (line plots). The approximations enabled calculations of pressure related quantities not only at particular flow rates at which pressures were measured, but in the entire flow range, thus enabling continuous representation of flow dependent uncertainties in the further analysis. As seen in Fig. 2, the differences between particular pressures get larger for flow rates higher than about 10 g/min, indicating more intense pressure oscillations during the prover's timing cycle.

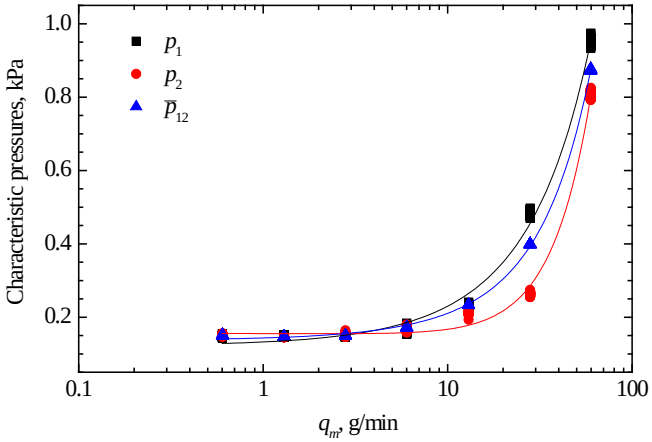

Fig. 2. The characteristic pressures in the timing cycles of the piston prover (measurement data and their approximations)

The connection volume is estimated to $V_d = 1.69 \cdot V_m^*$ having the standard uncertainty of $u(V_d) = 12.57\ \mathrm{cm^3}$, which covers the possible change of the connecting volume (connecting tubes with different lengths...). The adiabatic index γ for dry air equals 1.4 and is encompassed by a rectangular distribution having a half-width of 0.1 that leads to a standard uncertainty of $u(\gamma) = 0.1/\sqrt{3}$. The uncertainty contribution due to the temperature inhomogeneity in the cylinder was studied theoretically [15] and experimentally. It was established that the standard uncertainty of $u(\varepsilon_\rho^{\Delta T}) = 2 \cdot 10^{-4}$ can be attributed to this effect, if the maximum temperature difference between the inlet flow and the cylinder wall is 0.15 K below 6 g/min or up to 0.5 K at 60 g/min. It was proven that the required temperature difference can be assured by a proper temperature stabilization of the piston prover.

Fig. 3 displays the individual contributions and the resulting relative uncertainty of the density correction factor.

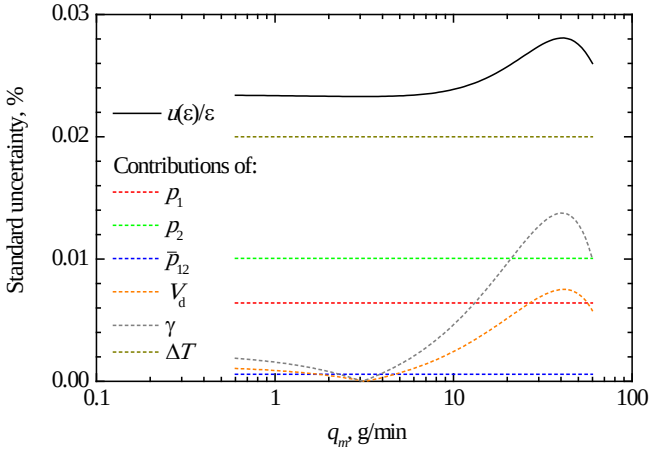

Fig. 3. Contributions to the uncertainty of the density correction factor

The value of $u(\varepsilon_\rho)/\varepsilon_\rho$ is about 0.023 % for the flow rates below 8 g/min, from where it increases to its peak value of 0.028 % at 40 g/min. The increase at higher flow rates is related to the increased difference between the pressures p_2 and p_1. It is also evident, that the largest contribution is due to the temperature inhomogeneity, whereas the contribution of $\overline{p}_{12}$ remains negligible in the entire flow range.

In Fig. 4 we compare the values of the density correction factors obtained by the adiabatic (5) and isothermal (6) measurement models. As already mentioned, the latter model is originally employed in the respective piston prover, whereas the former model was proven to be more accurate in our previous work [14]. The values of the correction factor in both cases are close to 1, but increase at higher flow rates. The absolute relative difference between the isothermal and the adiabatic model $\delta_\varepsilon = \left|(\varepsilon_\rho^{(T)} - \varepsilon_\rho^{(A)})/\varepsilon_\rho^{(A)}\right|$, which is also shown in Fig. 4, is close to zero at the low end of the observed flow range, but increases above 0.05 % for flow rates greater than 10 g/min (up to 0.13 % at 40 g/min), which coincides with the range of increased pressure oscillations.

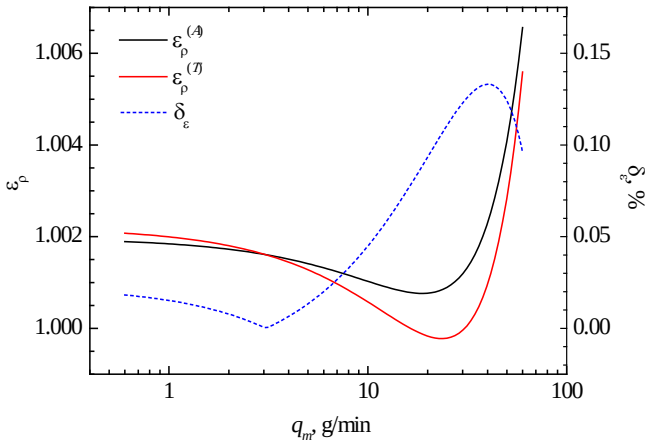

Fig. 4. Values of the density correction factor ε_ρ for the adiabatic and the isothermal model and their relative difference δ_ε

3.5. Repeatability

In order to evaluate the repeatability, the piston prover was connected to the stable gas flow source and then fifty consecutive readings were taken at each of seven different mass flow rates. Fig. 5 presents the repeatability estimated as the experimental standard deviation, $s(q_m)$, of: (i) single measurements, (ii) ten moving-averaged (consecutive) measurements. A single measurement (reading) is a value obtained from a single measurement cycle of the piston prover. The results show that averaging ten consecutive readings of the piston prover decreases the experimental standard deviation in average by almost a factor from 3 to 4.

Based on the experimental data, the following values for repeatability were considered in the uncertainty analysis: (i) 0.02 % up to 10 g/min from where it linearly increases up to 0.04 % at 60 g/min for a measurement result obtained by a single measurement and (ii) a constant value of 0.01 % for the average value of ten consecutive readings.

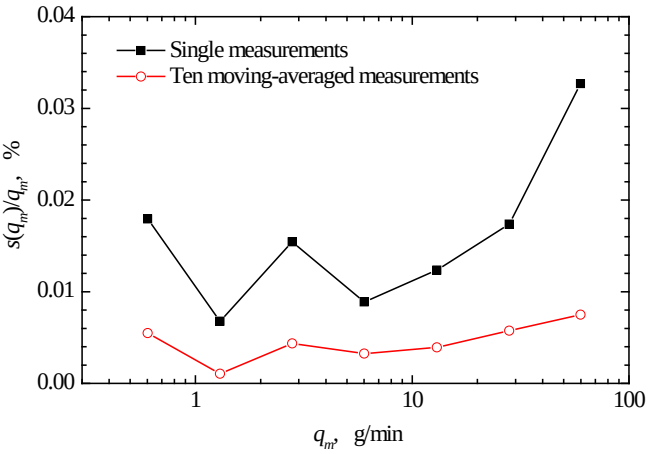

Fig. 5. The experimental standard deviation calculated for (i) single measurements, (ii) ten moving-averaged measurements

3.6. Combined and expanded uncertainty

Using the contributions of individual components presented in this Section, the combined standard uncertainty of the mass flow rate can be expressed by combining the components listed in Table 4 (considering $q_{v,l}^{(p)} << V_m^*/\Delta t$ in the notation of the sensitivity coefficients).

Table 4. Components of the combined mass flow rate uncertainty,

$$u(q_m)/q_m = \sqrt{\sum_i \left(c_{rel,i}\, u(x_i)/x_i\right)^2}$$

x_i	$c_{rel,i}\, u(x_i)/x_i$
ρ	$u(\rho)/\rho$
$V_m^*/\Delta t$	$u(V_m^*/\Delta t)/(V_m^*/\Delta t)$
ε_ρ	$u(\varepsilon_\rho)/\varepsilon_\rho$
$q_{v,l}^{(p)}$	$u(q_{v,l}^{(p)})/(V_m^*/\Delta t)$
repeatability	$s(q_m)/q_m$

Fig. 6 shows the combined uncertainty of the mass flow rate obtained as a single reading by applying the adiabatic model for the density error correction. The contributions of particular components listed in Table 4 are also presented in the graph. In the considered case the combined uncertainty is in the range between 0.06 % and 0.07 %. A slight increase of the uncertainty below 1 g/min can be attributed to the leakage flow component, whereas the increase at highest flow rates is caused mainly by the augmented repeatability. The most important uncertainty contribution is due to the determination of the air density, which is not related to the flow rate and is therefore constant.

On the other hand, if the mass flow rate is determined by averaging ten consecutive readings, the repeatability does not represent a considerable contribution to the combined standard uncertainty. Thus, $u(q_m)/q_m$ becomes smaller or equal to 0.06 % in the entire flow range.

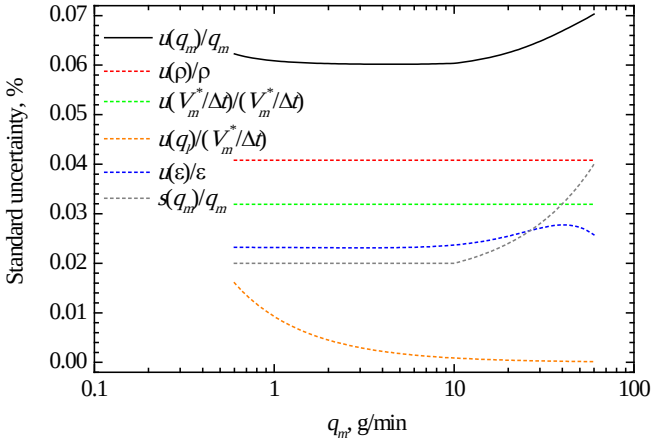

Fig. 6. Combined mass flow rate standard uncertainty including the contributions of individual components

The CMC of the piston prover is finally evaluated as the expanded measurement uncertainty of the mass flow rate $U(q_m)/q_m = k \cdot u(q_m)/q_m$ using the coverage factor, k, for 95.45 % confidence interval by taking into account the effective degrees of freedom, which are calculated according to the Welch-Satterthwaite formula [16]. In Fig. 7 we present $U(q_m)/q_m$ for three different cases. In the selected cases the mass flow rate was obtained by the following measurement methods: (i) as the average of ten consecutive readings using the adiabatic density correction factor, (ii) as a single reading using the adiabatic density correction factor and (iii) as the average of ten consecutive readings using the isothermal density correction factor. In the latter case the expanded uncertainty was evaluated by treating the relative difference between the isothermal and the adiabatic density correction factor, δ_ε, as the systematic error [16]: $U(q_m)/q_m = k \cdot u(q_m)/q_m + \delta_\varepsilon$.

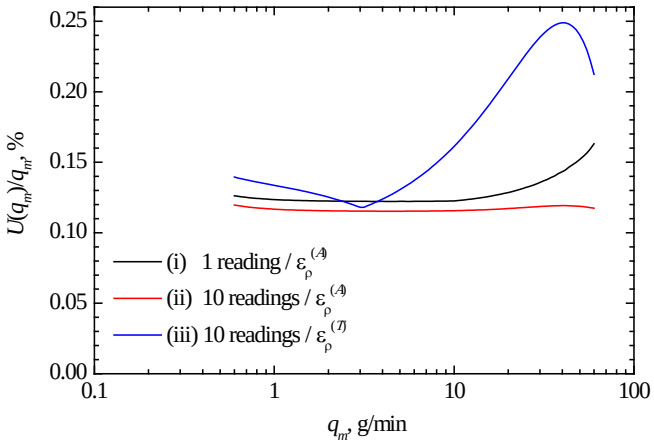

Fig. 7. Expanded mass flow rate uncertainty for three different measurement methods

The smallest CMC of the piston prover of 0.12 % for the flow cell under consideration is obtained when the measured value is calculated as the average of ten consecutive readings using the adiabatic density correction factor. Obtaining the measurement result as a single reading instead of an average of ten readings, the CMC is increased by a maximum of 0.01 % below 15 g/min and almost up to 0.05 % at 60 g/min. The observed difference in CMC at higher flows is related to the deteriorated repeatability and consequentially also to the higher values of the coverage factor that goes up to 2.3 at 60 g/min (in other two displayed cases $k = 2$). In the third case when the isothermal density correction factor is applied the uncertainty significantly increases above 5 g/min compared to other two cases and reaches its peak of 0.25 % at about 40 g/min. This is related to the increase of the absolute relative difference between the isothermal and adiabatic measurement model shown in Fig. 4.

4. CONCLUSIONS

The article discusses evaluation of the calibration and measurement capability (CMC) of the clearance-sealed piston prover. The paper presents the methodology of evaluating the uncertainty of the measured mass flow rate. The detailed analysis was presented for the measurement of dry air in the flow range between 0.6 g/min and 60 g/min.

The results of the uncertainty analysis show that the contributions of type B due to the measurements of the air density, the dimensional and the time quantities as well as the estimation of the density correction factor are of approximately same order of magnitude. At small flow rates also the influence of the leakage flow component becomes substantial and has to be considered. It was demonstrated that CMC of the piston prover can be reduced by determining the measured value as the average of multiple readings and by using the adiabatic model for the density correction factor. The implementation of the adiabatic instead of the isothermal density correction in the investigated version of the piston prover would require a use of an external fast response pressure gauge sensor. Adopting the listed measures it was shown that the CMC of the piston prover of 0.12 % of the measured value can be guaranteed in laboratory conditions.

REFERENCES

[1] J. D. Wright and G. E. Mattingly, *NIST Calibration Services for Gas Flow Meters – Piston Prover and Bell Prover Gas Flow Facilities*, Gaithersburg, MD: National Institute of Standards and Technology, 1998.

[2] J. D. Wright, G. E. Mattingly, S. Nakao, Y. Yokoi and M. Takamoto, "International comparison of a NIST primary standard with an NRLM transfer standard for small mass flow rates of nitrogen gas", *Metrologia*, Vol. 35, pp. 211–221, 1998.

[3] R. F. Berg and G. Cignolo, "NIST–IMGC comparison of gas flows below one litre per minute", *Metrologia*, Vol. 40, pp. 154–158, 2003.

[4] G. Cignolo, F. Alasia, A. Capelli, R. Goria and G. La Piana, "A primary standard piston prover for measurement of very small gas flows: an update", *Sensor Review*, Vol. 25, pp. 40–45, 2005.

[5] S. Sillanpää, B. Niederhauser and M. Heinonen, "Comparison of the primary low gas flow standards between MIKES and METAS", *Measurement*, Vol. 39, pp. 26–33, 2006.

[6] H. M. Choi, K.-A. Park, Y. K. Oh and Y. M. Choi, "Improvement and uncertainty evaluation of mercury sealed piston prover using laser interferometer", *Flow Measurement and Instrumentation*, Vol. 20, pp. 200–205, 2009.

[7] C.-M. Su, W.-T. Lin and S. Masri, “Establishment and verification of a primary low-pressure gas flow standard at NIMT”, *MAPAN – Journal of Metrology Society of India*, Vol. 26, pp. 173–186, 2011.

[8] R. F. Berg, T. Gooding and R. E. Vest, “Constant pressure primary flow standard for gas flows from 0.01 cm^3/min to 100 cm^3/min (0.007–74 μmol/s)”, *Flow Measurement and Instrumentation*, Vol. 35, pp. 84–91, 2014.

[9] Z.-P. Xu, J.-Y. Dai, H.-Y. Chen and D.-L. Xie, “Development of a reciprocating double-pistons gas prover”, *Flow Measurement and Instrumentation*, Vol. 38, pp. 116–120, 2014.

[10] M. P. van der Beek and R. van den Brink, “Gas Oil Piston Prover, primary reference values for Gas-Volume”, *Flow Measurement and Instrumentation*, In Press.

[11] H. Padden, “Uncertainty analysis of a high-speed dry piston flow prover”, *Measurement Science Conference*, Anaheim, CA, 2002.

[12] H. Padden, “Development of a 0.2% high-speed dry piston prover”, *Measurement Science Conference*, Anaheim, CA, 2003.

[13] J. Kutin, G. Bobovnik and I. Bajsić, “Dynamic effects in a clearance-sealed piston prover for gas flow measurements”, *Metrologia*, Vol. 48, pp. 123–132, 2011.

[14] J. Kutin, G. Bobovnik and I. Bajsić, “Dynamic pressure corrections in a clearance-sealed piston prover for gas flow measurements”, *Metrologia*, Vol. 50, pp. 66–72, 2013.

[15] J. Kutin, G. Bobovnik and I. Bajsić, “Dynamic temperature effects in a clearance-sealed piston prover for gas flow measurements”, *16th International Flow Measurement Conference (FLOMEKO)*, pp. 286–290, Paris, France, 2013.

[16] *JCGM 100:2008, Evaluation of Measurement Data – Guide to the Expression of Uncertainty in Measurement*, JCGM, 2008.

[17] E. W. Lemmon, M. L. Huber and M. O. McLinden, *NIST Reference Fluid Thermodynamic and Transport Properties—REFPROP Version 9.0*, MD: National Institute of Standards and Technology, Gaithersburg, 2010.

[18] A. Picard, R. S. Davis, M. Gläser and K. Fujii, ”Revised formula for the density of moist air (CIPM-2007)”. *Metrologia*, Vol. 45, pp. 149–155, 2008.